

Electrochemistry of rhodanine derivatives as model for new colorimetric and electrochemical azulene sensors for the detection of heavy metal ions

Ovidiu-Teodor Matica, Cornelia Musina (Borsaru), Alina Giorgiana Brotea, Eleonora-Mihaela Ungureanu, Mihaela Cristea, George-Octavian Buica and Alexandru C. Razus

Basic properties for the ligand R1 and characterization by elemental analysis, UV-Vis, ^1H NMR, ^{13}C -NMR, IR, MS

(Z)-5-(Azulen-1-ylmethylene)-2-thioxo-thiazolidin-4-one (R1), Dark brown crystals, it decomposes without melting. UV-Vis (MeOH), λ (log ϵ): 228 (4.07), 236 (4.07), 258 (4.07), 276 (4.05), 293 (3.95), 296 (3.95), 338 (3.82), 468 (4.47), 569 (3.09), 656 (2.80), 709 (2.55), 769 (2.56), 782 (2.57) nm. ^1H -NMR (300 MHz, DMSO, 25 °C): 7.53 [1 H, t, 3JH,H = 9.8, C(5')-H], 7.60 [1 H, t, 3JH,H = 9.8, C(7')-H], 7.64 [1 H, d, 3JH,H = 4.2, C(3')-H], 7.96 [1 H, t, 3JH,H = 9.8, C(6')-H], 7.99 [1 H, d, 3JH,H = 4.2, C(2')-H], 8.20 (1 H, s, CH=), 8.60 [1 H, d, 3JH,H = 9.4, C(4')-H], 8.94 [1 H, d, 3JH,H = 9.9, C(8')-H], 13.59 [1 H, s, NH] ppm; ^{13}C -NMR (75 MHz, DMSO, 25 °C): 119.1 (C-5), 122.0 (C-1'), 122.0 (C-3'), 123.7 (C-2'), 127.5 (C-7'), 128.2 (C-5'), 135.6 (CH=), 135.8 (C-8'), 139.2 (C-4'), 140.9 (C-6'), 140.9 (C-8a'), 144.1 (C-3a'), 169.4 (C-4), 194.8 (C-2) ppm. IR (neat): 490, 594, 655, 735, 775, 885, 957, 1092, 1176, 1232, 1284, 1333, 1371, 1397, 1483, 1613, 1706M, 2851, 2923, 3131 cm⁻¹. MS [ESI]: 272 [M+1]. Calcd. for $\text{C}_{14}\text{H}_9\text{NOS}_2$: C, 61.97; H, 3.34; N, 5.16; S. Found: C, 61.96; H, 3.37; N, 5.17.

Table S1. Equations of CV peak currents linear dependences on concentration for R2; the cathodic currents are in absolute values.

Process ¹	Equation	Adj. R-Square
a1	$ipa1 = 2.15 \times 10^{-5} + 1.91 \times 10^{-5} \times c$	0.996
a2	$ipa2 = 1.49 \times 10^{-6} + 2.58 \times 10^{-5} \times c$	0.998
a5	$ipa5 = 1.18 \times 10^{-4} + 8.67 \times 10^{-5} \times c$	0.935
c1	$ipc1 = 1.82 \times 10^{-5} + 6.35 \times 10^{-6} \times c$	0.577
c3	nlc ²	nlc ²

¹a3, a4 and c2 process have shoulders, and the peak value can't be evaluated.² nonlinear correlation

Table S2. Equations of DPV peak currents linear dependences on concentration for R2; the cathodic currents are in absolute values.

Process ¹	Equation	Adj. R-Square
a1	$ipa1 = 9.1 \times 10^{-7} + 8.54 \times 10^{-6} \times c$	0.999
a2	$ipa2 = -2.29 \times 10^{-8} + 8.16 \times 10^{-6} \times c$	0.999
a4	$ipa4 = 3.83 \times 10^{-6} + 4.87 \times 10^{-6} \times c$	0.968
a5	$ipa5 = 6.18 \times 10^{-6} + 1.01 \times 10^{-6} \times c$	0.998
c1	$ipc1 = 2.95 \times 10^{-7} + 5.61 \times 10^{-6} \times c$	1.000
c3	$ipc3 = 5.05 \times 10^{-6} + 1.69 \times 10^{-5} \times c$	0.983

¹a3 and c2 process have shoulders, and the peak value can't be evaluated.

Table S3. Calculated r/m ratios for $(\text{Pb})_m(\text{R1})_r$ from absorbance (A) values according to Mollard method.

Crit. No.	Excess of Pb			Excess of Ligand			r/m	m	r	Complex formula
	[Pb]/[R1]	[R1], μM	A	[Pb]/[R1]	[Pb], μM	A				
1	5/1	12.069	0.341	0.4/1	5.230	0.346	2.041	1	2.04	PbR1 ₂
2	4.5/1	12.143	0.388	0.4/1	5.230	0.346	2.107	1	2.11	PbR1 ₂
3	4/1	12.217	0.376	0.4/1	5.230	0.346	2.190	1	2.19	PbR1 ₂
4	3.5/1	12.292	0.369	0.4/1	5.230	0.346	2.244	1	2.24	PbR1 ₂
5	3.5/1	12.292	0.369	0.5/1	6.529	0.339	1.730	1	1.73	PbR1 ₂
6	3/1	12.368	0.348	0.5/1	6.529	0.339	1.847	1	1.85	PbR1 ₂
7	2.5/1	12.445	0.355	0.5/1	6.529	0.339	1.820	1	1.82	PbR1 ₂
8	5/1	12.069	0.341	0.7/1	9.117	0.330	1.096	1	1.10	PbR1
9	5/1	0.398	0.341	0.8/1	5.230	10.406	0.944	1	0.94	PbR1
10	4.5/1	12.143	0.388	0.8/1	5.230	10.406	0.974	1	0.97	PbR1
11	4/1	12.217	0.376	0.8/1	5.230	10.406	1.013	1	1.01	PbR1
12	3.5/1	12.292	0.369	0.8/1	5.230	10.406	1.038	1	1.04	PbR1
13	3.5/1	12.292	0.369	0.9/1	11.692	0.320	0.912	1	0.91	PbR1
14	3/1	12.368	0.348	0.9/1	11.692	0.320	0.974	1	0.97	PbR1
15	2.5/1	12.445	0.355	0.9/1	11.692	0.320	0.960	1	0.96	PbR1

Table S4. Calculated r/m ratios for $(\text{Pb})_m(\text{R2})_r$ from absorbance (A) values according to Mollard method.

Crit. No.	Excess of Pb			Excess of Ligand			r/m	m	r	Complex formula
	[Pb]/[R2]	[R2], μM	A	[Pb]/ [R2]	[Pb], μM	A				
1	3/1	5.438	0.235	0.5/1	2.756	0.276	2.316	1	2.32	PbR2 ₂
2	3/1	5.438	0.235	0.6/1	3.306	0.263	1.840	1	1.84	PbR2 ₂
3	2.5/1	5.453	0.232	0.5/1	2.756	0.276	2.352	1	2.35	PbR2 ₂
4	2.5/1	5.453	0.232	0.6/1	3.306	0.263	1.869	1	1.87	PbR2 ₂
5	2/1	5.468	0.231	0.5/1	2.756	0.276	2.369	1	2.37	PbR2 ₂
6	2/1	5.468	0.231	0.6/1	3.306	0.263	1.883	1	1.88	PbR2 ₂
7	1.8/1	5.474	0.229	0.5/1	2.756	0.276	2.394	1	2.39	PbR2 ₂
8	1.8/1	5.474	0.229	0.6/1	3.306	0.276	1.903	1	1.90	PbR2 ₂
9	1.5/1	5.483	0.231	0.5/1	2.756	0.263	2.378	1	2.38	PbR2 ₂
10	1.5/1	5.483	0.231	0.6/1	3.306	0.276	1.890	1	1.89	PbR2 ₂
11	3/1	5.438	0.235	1/1	5.498	0.236	0.995	1	0.99	PbR2
12	2.5/1	5.453	0.232	1/1	5.498	0.236	1.011	1	1.01	PbR2
13	2/1	5.468	0.231	1/1	5.498	0.236	1.018	1	1.02	PbR2
14	1.8/1	5.474	0.229	1/1	5.498	0.236	1.029	1	1.03	PbR2
15	1.5/1	5.483	0.231	1/1	5.498	0.236	1.022	1	1.02	PbR2

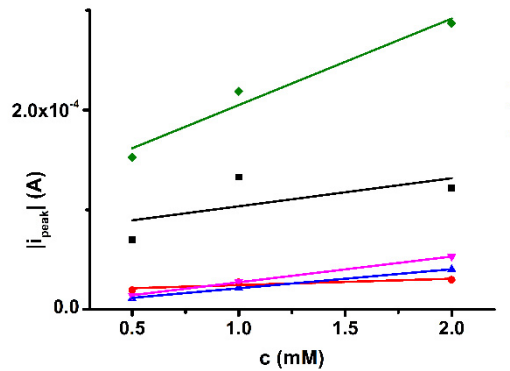


Figure S1. Dependences of the CV peak currents (at the scan rate of 0.1 Vs^{-1}) vs. R2 concentration (c); the cathodic currents are in absolute value.

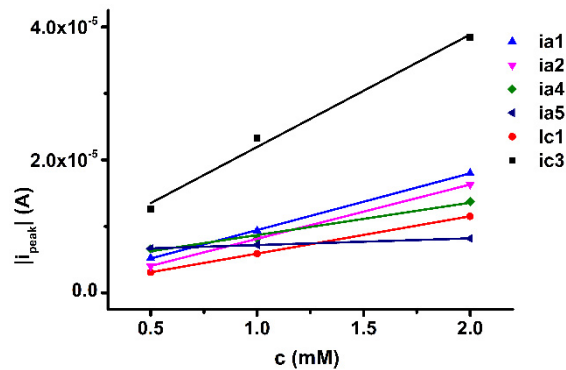


Figure S2. Dependences of peak currents for DPV vs. R2 concentration (c); the cathodic currents are in absolute value.

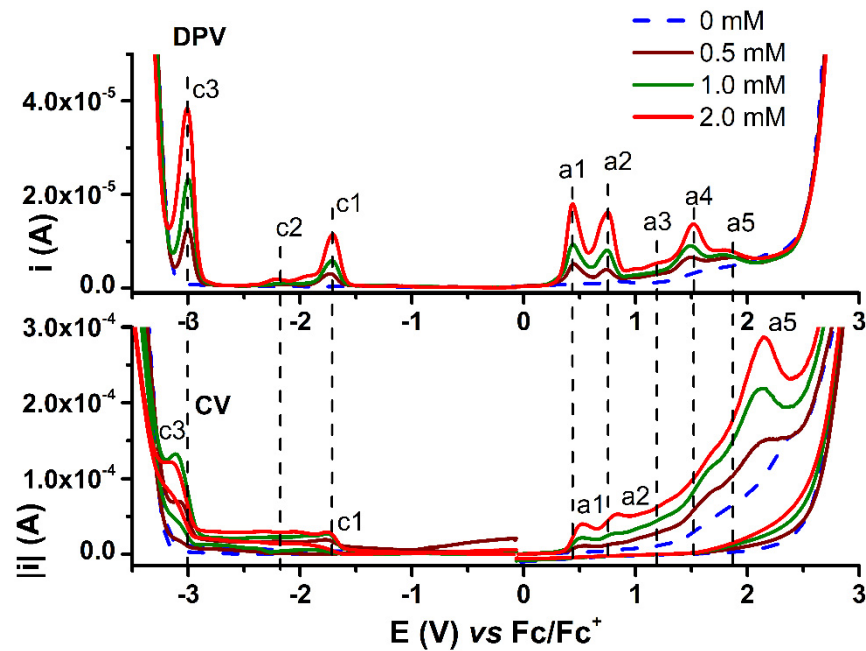


Figure S3. DPV and CV (0.1 V/s) curves on GC for R2 at different concentrations (mM) in $0.1 \text{ M TBAP/CH}_3\text{CN}$; the cathodic currents are in absolute value.

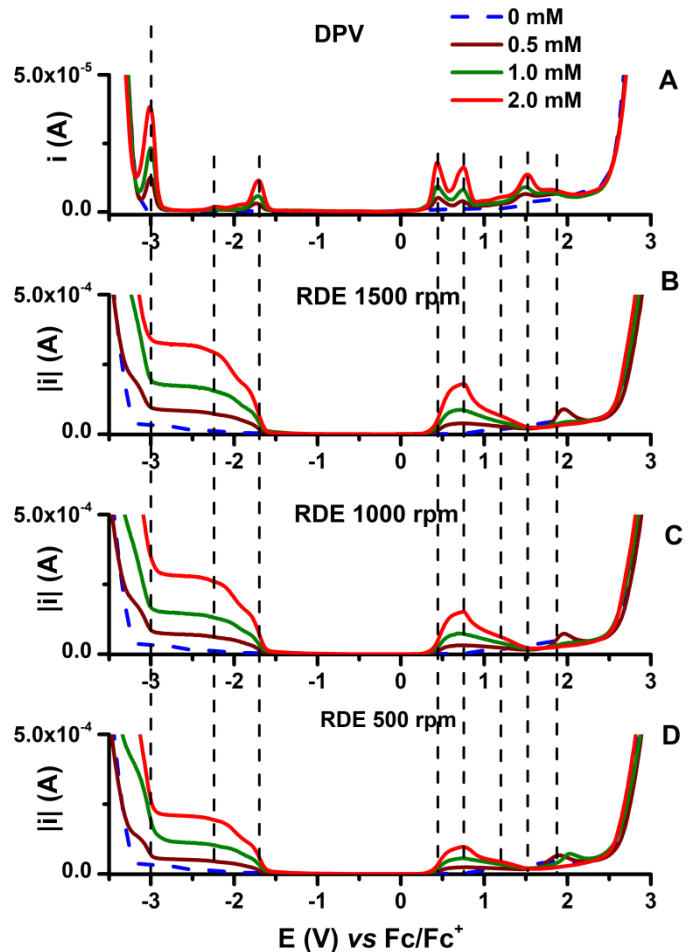


Figure S4. DPV (0.01 V/s) (A), RDE at 1500 rpm (B), RDE at 1000 rpm (C), and RDE 500 rpm(D) curves (with currents in absolute values) on GC for **R2** in 0.1 M TBAP/ CH₃CN at different concentrations (mM): 0 (dashed blue line), 0.5 (wine line), 1 (olive line), 2 (red line).

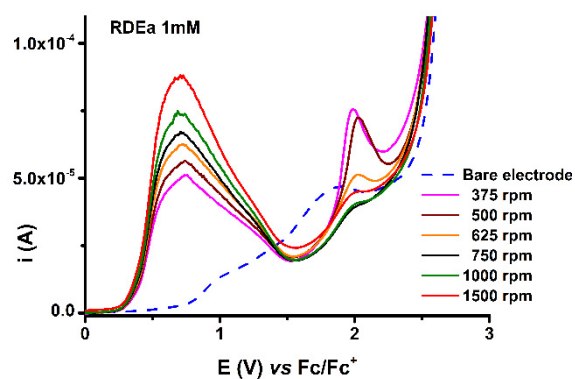


Figure S5. Anodic RDE curves on GC at different rotation rates (rpm) for $[R2] = 1$ mM in 0.1M TBAP/ CH₃CN.

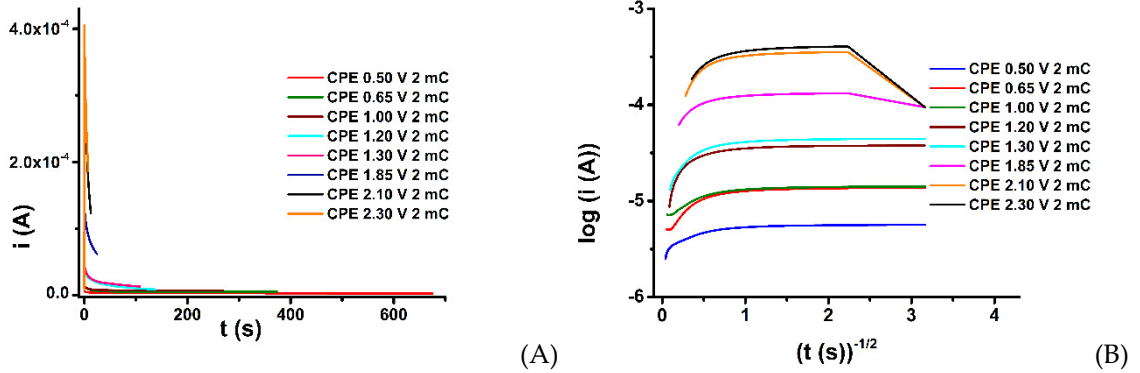


Figure S6. Chronoamperograms in coordinates i - t (A) and $\log(i)$ - $t^{-1/2}$ (B) during the preparation of R2-CMEs by CPE at different potentials using charges of 2 mC.

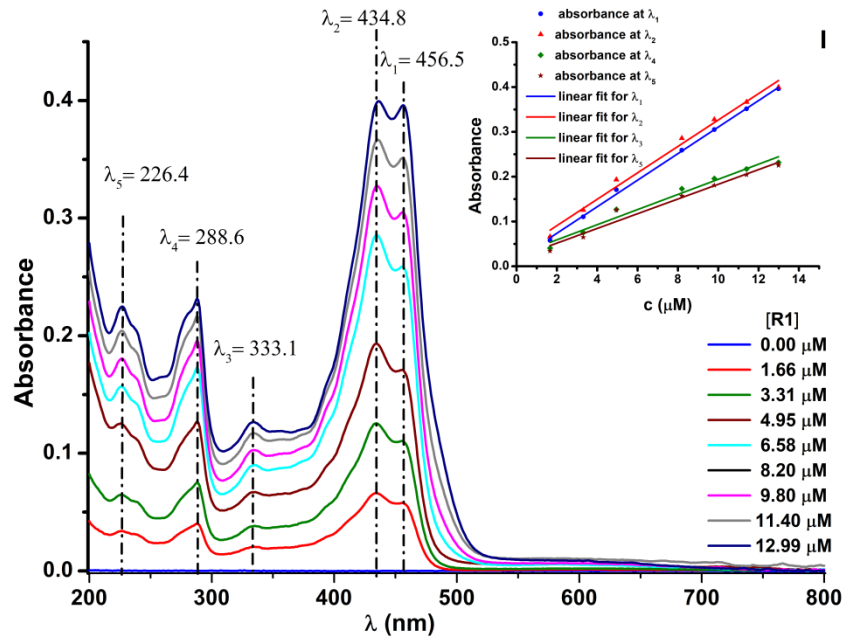


Figure S7. UV-Vis spectra obtained for different concentrations of R1 and inset: dependence of absorbances on R1 concentration (c).

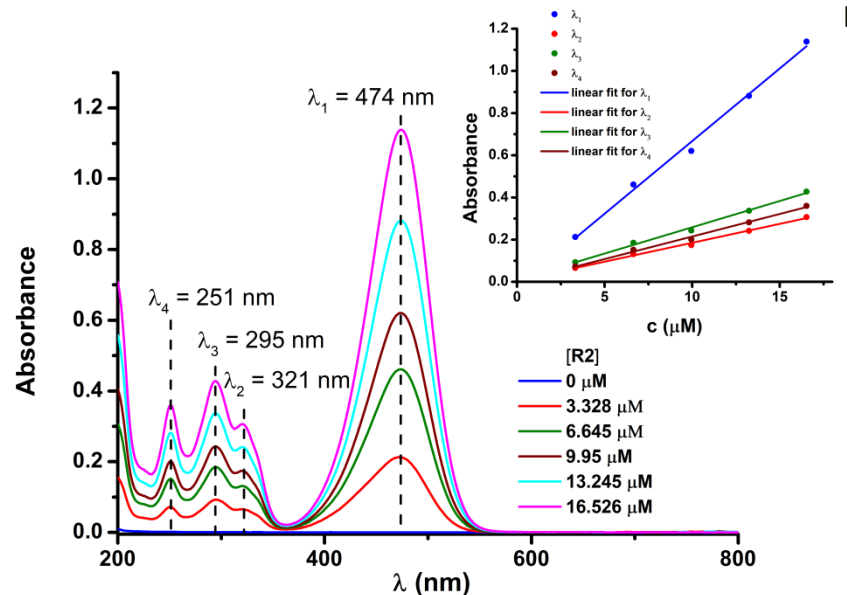


Figure S8. UV-Vis spectra obtained for different concentrations of R2 and inset: dependence of absorbances on R2 concentration (c).